Journal of Alloys and Compounds 785 (2019) 110–116

Contents lists available at ScienceDirect

Journal of Alloys and Compounds

journal homepage: http://www.elsevier.com/locate/jalcom

A novel way to synthesize nitrogen doped porous carbon materials with high rate performance and energy density for supercapacitors

Xin Hu [1], YaHui Wang [1], Bing Ding, Xiaoliang Wu*

Department of Chemistry, College of Science, Northeast Forestry University, 26 Hexing Road, Harbin, 150040, PR China

ARTICLE INFO

Article history:
Received 17 November 2018
Received in revised form
11 January 2019
Accepted 13 January 2019
Available online 14 January 2019

Keywords:
Nitrogen doped porous carbon
Agar
Potassium citrate
Supercapacitors

ABSTRACT

We report a novel, facile method for the synthesis of nitrogen doped porous carbon with three-dimensional interconnected porous framework by one-step pyrolysis of the mixture of agar, potassium citrate and urea. The optimized material possesses large specific surface area, interconnected porous framework and massive heteroatom functional groups. As an electrode material, it delivers a high specific capacity of 357 F g^{-1} at 1 A g^{-1}, good rate performance (267 F g^{-1} at 50 A g^{-1}) and good electrochemical stabilization (95.6% initial capacitance retained after 10,000 cycles) in 6 M KOH solution. Moreover, the as-prepared symmetric supercapacitor based on the NPC electrodes shows an energy density of 24.1 Wh Kg^{-1} between the voltage ranges of 0–1.8 V in 1 M Na_2SO_4 solution, comparable with most of reported carbon-based symmetric supercapacitors. More immortally, even at a high power density of 12.5 kW kg^{-1}, it still remains an energy density of 12.5 Wh kg^{-1}. Therefore, this paper provides a facile, sustainable method for the synthesis of heteroatom doped three-dimensional interconnected porous carbon materials for high performance supercapacitors.

1. Introduction

Supercapacitors are considered as an important class of energy storage system because of their ultrahigh power density, fast charge-discharge feature, excellent cyclic performance and environmentally friendly feature [1–5]. Among different electrode materials, porous carbon materials are the most commonly used as electrode materials for electrochemical double layer capacitors owing to their large surface areas, massive raw materials, tunable pore structure and excellent chemical stability [6–9].

Porous carbon materials usually can be obtained from fossil or biological materials (such as coal, wood and coconut shells) by carbonization in inert gas followed by physical or chemical activation [10–13]. Consequently, the electrochemical characteristics of the porous carbon mightily rely on activating method and precursor instinct. Using KOH, NaOH, $ZnCl_2$ as activating agents are conventional method to synthesize porous carbon for electrode materials of supercapacitor. However, the manufacturing process is complex and these activating agents are highly corrosive to instrumentation, which are not advantageous for the large-scale production [14]. Given this, researchers try to direct pyrolysis of metal organic salts without extra activating agent, which opens up a new way to synthesize novel porous carbon materials, for example citrates [6], potassium tartrate [15] and gluconates [16]. On the other hand, porous carbon obtained from conventional method usually suffers from large ion diffusion resistance and long ion diffusion distance, resulting unsatisfactory specific capacitance and poor rate performance [17,18].

Recently, heteroatoms doped three-dimensional (3D) interconnected porous carbon materials are emerging as a new class of promising electrode materials for supercapacitor [19–21]. The 3D interconnected porous structure can not only offer available high specific surface area to adsorb massive electrolyte ion, but also reduce ion diffusion resistance, which has attracted significant attentions [19,22]. Moreover, heteroatoms doping is regarded as an effective way to ameliorate the hydrophilicity and conductivity of porous carbon materials. Particularly for nitrogen atoms, the difference in electronegativity between the N and C atoms can offers a more polarized interface, resulting improve the hydrophilicity of the carbon materials. Additionally, the nitrogen functional groups can provide extra pseudocapacitances via redox reaction [23–25].

Herein, we develop a facile strategy for the synthesis of nitrogen doped porous carbon (NPC) with 3D interconnected porous architecture by one-step pyrolysis of the mixture of agar, potassium

* Corresponding author.
E-mail address: wuxiaoliang90@163.com (X. Wu).
[1] Co-first authors.

https://doi.org/10.1016/j.jallcom.2019.01.160
0925-8388/

citrate and urea. Benefitting from the large specific surface area (1300 $m^2 g^{-1}$), 3D interconnected porous framework and heteroatoms functional groups, the NPC electrode delivers large specific capacity (357 $F g^{-1}$ at 1 $A g^{-1}$), good rate property (267 $F g^{-1}$ at 50 $A g^{-1}$) and impressive electrochemical stabilization (95.6% initial capacitance retained after 10,000 cycles) in 6 M KOH aqueous electrolyte. More interestingly, the as-fabricated symmetric supercapacitor based on NPC electrodes shows an energy density of 24.1 Wh Kg^{-1} in 1 M Na_2SO_4 aqueous solution.

2. Experimental section

2.1. Synthesis of nitrogen doped porous carbon materials

Agar (1 g), urea (1 g) and potassium citrate (1 g) were added into 20 mL distilled water, then heated up to 85 °C with violent stirring. Then, the mixtures were dried in oven. The obtained samples were pyrolyzed at 700 °C for 2 h in a tube furnace under N_2 flow with a heating rate of 3 °C min^{-1}. The resulting materials were washed by dilute HCl solution and distilled water, dried in oven at 90 °C for 12 h. The obtained product was denoted as NPC. For comparison, samples were prepared according to the NPC without urea, and the obtained sample was denoted as PC. In addition, sample was prepared according to the NPC without urea and potassium citrate, and the product was denoted as AC.

2.2. Characterization methods

The microstructure was characterized by scanning electron microscope (SEM, JEOL JSM-7500F) and transmission electron microscope (TEM, JEOL JEM2010). The crystallographic feature was checked by X-ray diffraction (XRD). Raman spectra were determined by a Jobin-Yvon HR800 spectrometer at an excitation wavelength of 458 nm. Thermogravimetric analysis (TGA) was conducted on a PerkineElmer Diamond thermal analyzer. X-ray photoelectron spectroscopy (XPS) analysis was collected on a PHI5700ESCA spectrometer using a monochromatic (Kα radiation) source. The pore characteristic was measured by nitrogen adsorption/desorption through the BET method and pore size distribution were computed by density functional theory (DFT).

2.3. Electrochemical measurements

The electroactive materials, carbon black, tetrafluoroethylene were mixed in ethanol at 75:20:5 by mass ratio to obtain slurry. The slurry pasted onto the Ni foam (1 cm × 1 cm) and dried in oven. The mass loading of the electrode materials was about 3 mg cm^{-2}. Cyclic voltammetry and galvanostatic charge-discharge measurements of the three-electrode system were recorded between −1 and 0 V (vs. Hg/HgO). Electrochemical impedance spectra were tested from a frequency range of 0.01 Hz–100 kHz at an AC amplitude of 5 mV. The symmetrical device was prepared with two NPC electrodes with the equal mass and separated by a glassy fibrous separator. All the electrochemical tests were recorded by a CHI 660E electrochemical workstation.

The specific capacity of the three-electrode system was computed by the following formula:

$$C = \frac{I\Delta t}{m\Delta V} \quad (1)$$

where I is the current density, Δt is the discharge time, ΔV is the voltage window, and m is the weight of the electroactive materials.

The specific capacity, energy density (E) and power density (P) of the symmetrical device were computed by the following formulas:

$$C = \frac{\int IdV}{\nu m V} \quad (2)$$

$$E = 0.5CV^2 \quad (3)$$

$$P = E/\Delta t \quad (4)$$

where I is the current density, V is the voltage window, ν is the scan rate, m is the weight of the active materials of the two electrodes and Δt is the discharge time (s).

3. Results and discussion

The microstructures of the as-prepared materials were firstly checked by scanning electron microscopy (SEM). As shown in Fig. S1a, the AC samples show irregular block structure without obvious pores. For the PC sample, it shows obviously porous structure with micrometer-sized macropore. With increasing ratio of potassium citrate to Agar, the pore size of the as-prepared samples becomes bigger (Figs. S1b–d). Significantly, similar with PC, SEM images of NPC (Fig. 1a, b) show 3D interconnected porous structure with randomly opened pores ranging from 0.2 to 1.0 micrometers. These sub-micrometer sized pores can act as ion-buffering reservoir to offer short transport route for electrolyte ions. Furthermore, the corresponding element mapping images of NPC demonstrate the uniform distribution of C (Fig. 1d), O (Fig. 1e), and N (Fig. 1f). Transmission electron microscope (TEM) image of NPC further confirms the 3D interconnected porous structure (Fig. 1g). Significantly, high-resolution TEM image (Fig. S1c) shows a great deal of micropores in the carbon walls, which in favor of the energy storage for supercapacitors [26]. The generation of micropores is due to the activation of carbon precursors by potassium/potassium oxide from the decomposition of citrate potassium, which is confirmed by TG analysis (Fig. S2). First, when the temperature is less than 500 °C, decomposition of potassium citrate to produce potassium carbonate and then the product decomposed at higher temperatures ($K_2CO_3 \rightarrow CO_2 + K_2O$). Metallic potassium is produced via the reduction of K_2O by carbon ($K_2O + C \rightarrow 2K + CO$).

The crystal structures of the obtained materials were checked by X-ray diffraction (XRD). As shown in Fig. 2a, all the samples display two wide diffraction peaks at around 24° and 43°, which ascribed to the (002) and (101) crystal planes of the carbon material, respectively. Contrasting with PC sample, the reduced height of the (002) peak for NPC implies the increasing disorder structure owing to gas release from during urea pyrolysis process. The disordered features of obtained samples were further confirmed by Raman spectroscopy analysis (Fig. 2b). The intensity ratio of the D and G bands (I_D/I_G) of the NPC (1.03) is higher than PC-700 (0.98), revealing that the NPC sample possesses more defects and disordered graphite [27–29].

The surface characterizations of the obtained porous materials were conducted by X-ray photoelectron spectra (Fig. 2c). The XPS analytic result reveals that the contents of O and N are 9.7 and 2.4 at.% in NPC, which can generate some pseudocapacitance during the charge/discharge process. Additionally, the high-resolution XPS of C (Fig. 2d) exists five different peaks at 284.2, 284.8, 286.2, 287.0 and 289.1 eV, which can be ascribed to the C-C, C-N, C-O, C=O, and O-C=O, respectively [30,31]. The pore structures of the as-prepared samples were investigated by N_2 adsorption/desorption isotherms measurements. As shown in Fig. 3a, all the materials show the feature of type I isotherms, which the adsorption capacity

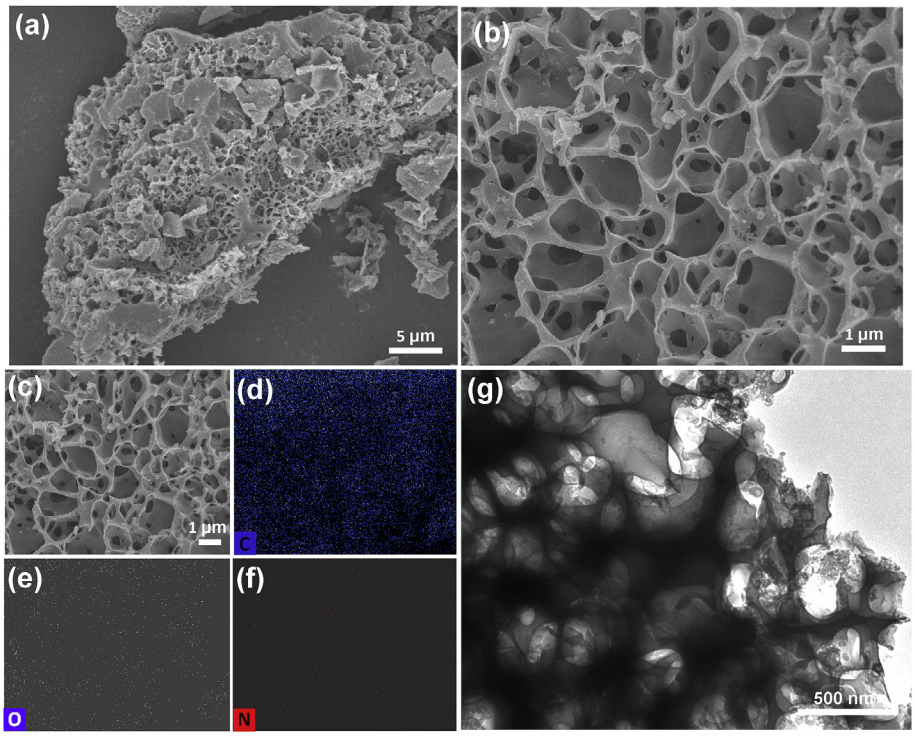

Fig. 1. (**a**, **b**) SEM images of NPC (**c**) SEM image of NPC, and corresponding elemental mapping images of C (**d**), O (**e**), N (**f**). (**g**) TEM image of NPC.

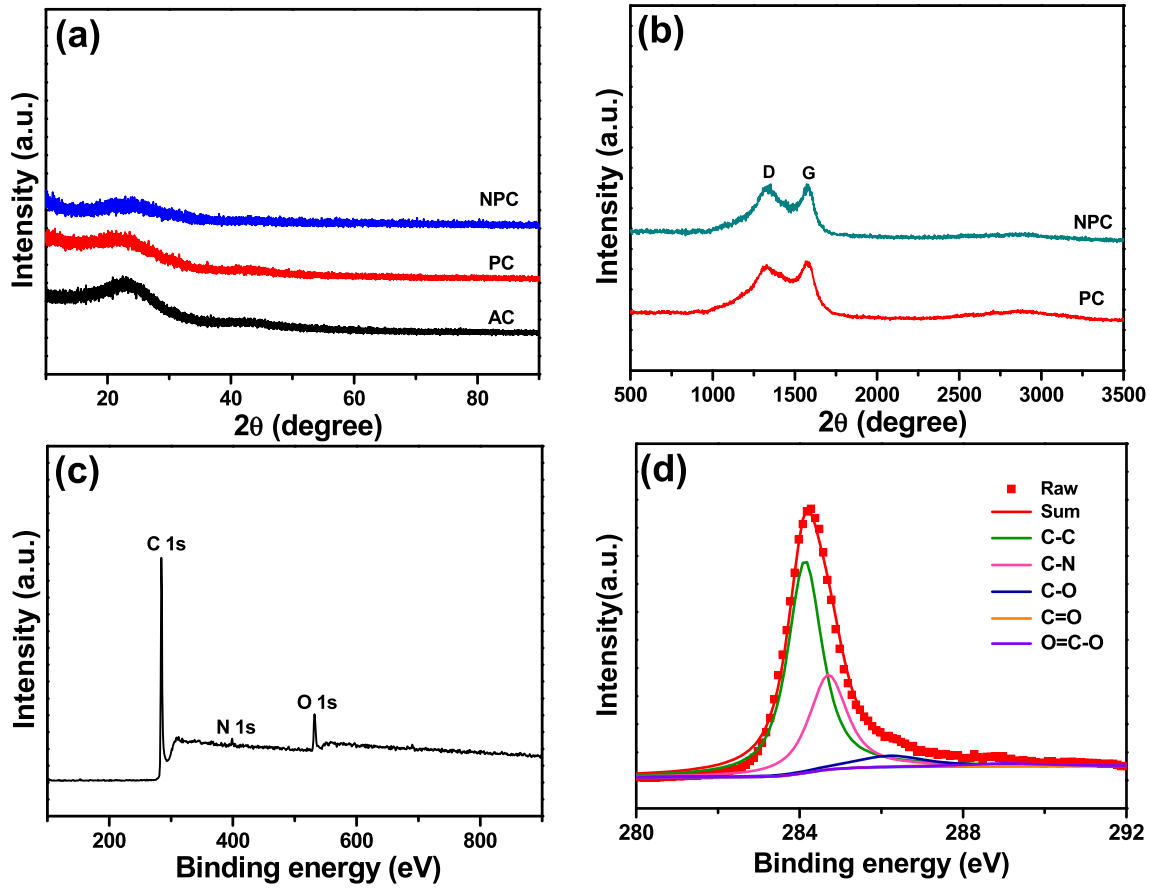

Fig. 2. (**a**) XRD patterns of the AC, PC and NPC samples. (**b**) Raman spectrum of the PC, NPC samples. (**c**) XPS survey spectrum of the AC, PC and NPC samples. **(d)** High-resolution C 1s of NPC sample.

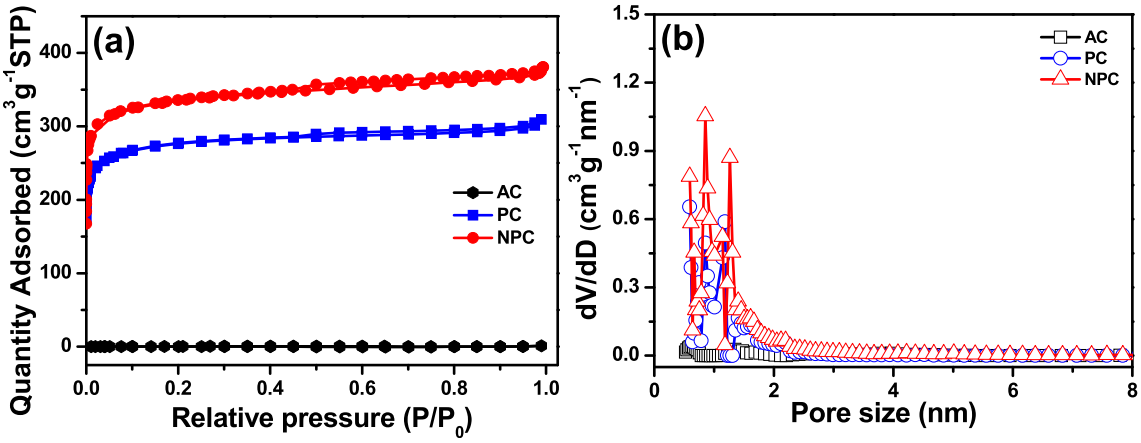

Fig. 3. (**a**) N_2 adsorption/desorption isotherms of the AC, PC and NPC samples. (**b**) Pore sizes distribution of the NPC sample.

increased sharply at relatively small pressure can be observed owing to micropores filling. The NPC material exhibits a high surface area of 1300 $m^2 g^{-1}$, higher than AC (10 $m^2 g^{-1}$) and PC (1070 $m^2 g^{-1}$). Fig. 3b shows the pore size distribution of the porous carbon. It can be clearly found that NPC samples possess massive micropores with peaks centered at 0.85 and 1.30 nm, which is in favor of energy storage for supercapacitors.

Owing to its 3D interconnected porous framework, large specific surface area and high heteroatom functional groups, the NPC materials are expected to be as the outstanding candidate for the construction of excellent performance supercapacitors. The electrochemical characteristics of the as-prepared materials were firstly performed by CV in 6 M KOH electrolyte with a three-electrode system. Fig. 4a exhibits the CV curves of the AC, PC and NPC samples at 50 mV s^{-1}. Contrasting with the PC samples, CV profile of the NPC sample exhibits obvious Faradaic humps, indicating that more contribution comes from redox reaction for NPC. Notably, the integral area of CV profile of the NPC samples is larger than other samples, corresponding to a larger specific capacity because of its large specific surface area, 3D interconnected porous framework and high heteroatom functional groups. High content of nitrogen and oxygen functional groups can not only improve the wettability of carbon surface, but also provide additional pseudocapacitance. It can be found that the CV curve (Fig. 4b) of NPC displays rectangular-like profile at a high scan rate of 500 mV s^{-1}, showing that good rate performance due to its 3D interconnected

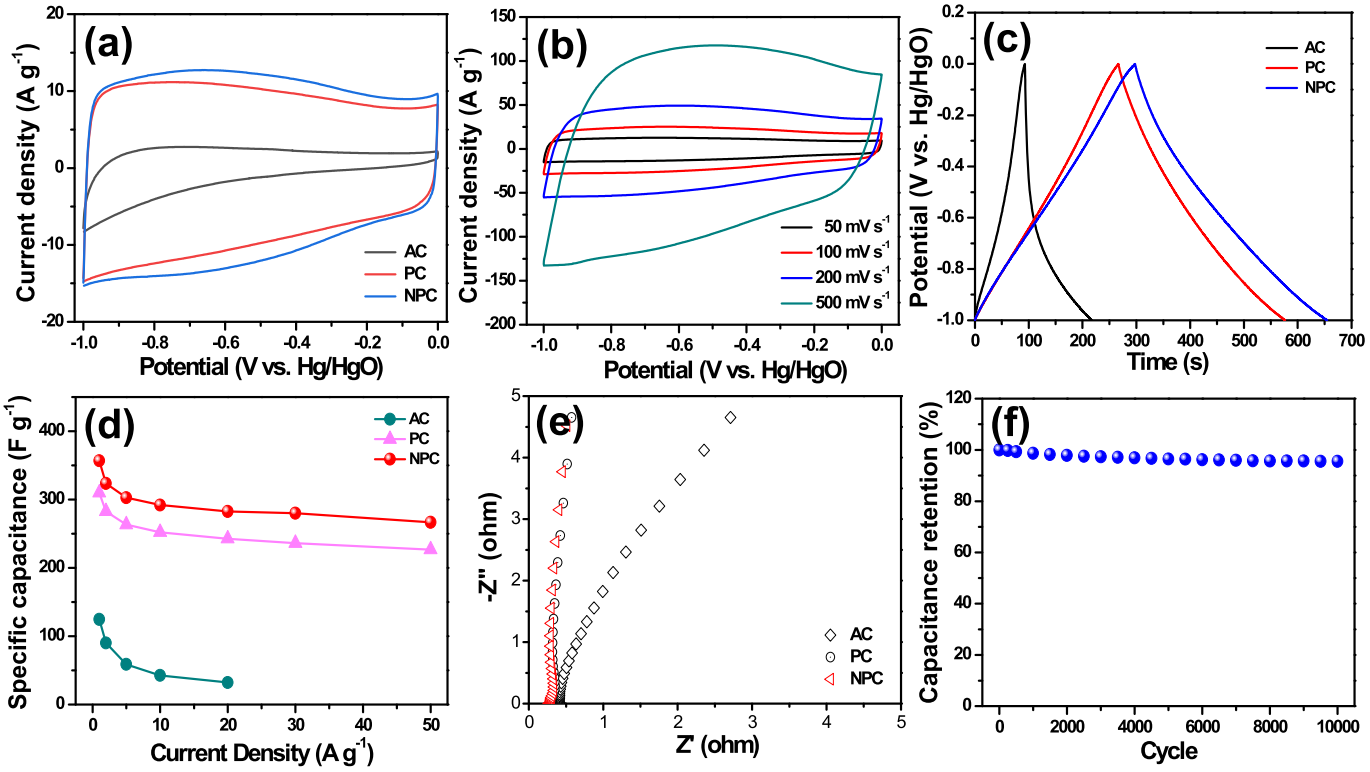

Fig. 4. (**a**) CV curves of the AC, PC and NPC electrodes at a scan rate of 50 mV s^{-1}. (**b**) CV curves of the NPC electrodes at different scan rates. (**c**) Galvanostatic charge/discharge curves of the AC, PC and NPC electrodes at 1 A g^{-1}. (**d**) Specific capacitance of the AC, PC and NPC electrodes at different current densities. (**e**) Nyquist plots of the AC, PC and NPC electrodes. (**f**) Electrochemical stability of the NPC electrode tested at a scan rate of 200 mV s^{-1} for 10,000 cycles.

Table 1
Summary of electrochemical performance for carbon electrode materials.

Material	C (F g^{-1})	Electrolyte	Ref.
Coal derived hierarchical porous carbon	304 (1.0 A g^{-1})	6 M KOH	[9]
Fallen leaves derived hierarchical porous carbon	242 (0.3 A g^{-1})	6 M KOH	[13]
Banana peel derived hierarchical porous carbon	206 (1.0 A g^{-1})	6 M KOH	[21]
Soybean derived nitrogen-doped carbons	243 (0.5 A g^{-1})	6 M KOH	[32]
Glucose derived nitrogen-doped porous carbon	293 (1.0 A g^{-1})	6 M KOH	[33]
Soybean derived nitrogen-doped carbons	215 (0.5 A g^{-1})	2 M KOH	[34]
Chitosan derived nitrogen-doped porous carbon	252 (0.5 A g^{-1})	6 M KOH	[35]
Bagasse derived hierarchical porous carbon	260 (0.1 A g^{-1})	6 M KOH	[36]
Chicken eggshell membranes derived carbon	297 (0.2 A g^{-1})	1 M KOH	[37]
Coconut shell sheet-like graphitic carbon	268 (1.0 A g^{-1})	6 M KOH	[38]
Auricularia derived carbon	196 (5.0 mV s^{-1})	6 M KOH	[39]
N-doped 3D graphitic foam	330 (5.0 mV s^{-1})	6 M KOH	[40]
NPC	**357 (1.0 A g^{-1})**	**6 M KOH**	**This work**

porous framework ensuring rapid ion diffusion. Furthermore, the NPC sample exhibits a longer charge-discharge time than the AC and PC electrodes at 1 A g^{-1} (Fig. 4c). The NPC electrode exhibits a specific capacity of 357 F g^{-1} at 1 A g^{-1} (Fig. 4d), which is comparable with those of AC electrode (124 F g^{-1} at 1 A g^{-1}) and PC electrode (309 F g^{-1} at 1 A g^{-1}) and other previously published carbon-based materials (Table 1). Significantly, the NPC electrode still shows a specific capacity of 267 F g^{-1} even at a high current density of 50 A g^{-1}, suggesting excellent rate property. From the Nyquist plots in Fig. 4e, NPC exhibits a smaller equivalent series resistance (0.27 Ω) than AC (0.29 Ω) and PC (0.42 Ω), meaning a better conductivity for NPC. The electrochemical stabilization of the NPC electrode was tested by cyclic voltammetry measurement at 200 mV s^{-1}. As shown in Fig. 4f, the NPC electrode maintains 95.5% of the initial capacity after running 10,000 cycles, meaning good electrochemical stabilization.

To further characterize the practical electrochemical properties of the NPC materials, two-electrode symmetric supercapacitor based on the NPC samples was fabricated. It is worth noting that energy density of supercapacitors is not only related to its specific capacity, but also to the voltage window. As reported by literature [41], Na_2SO_4 electrolyte can provide larger voltage range than acid and alkaline ones, in favor of large energy density. Therefore, the NPC//NPC symmetric supercapacitor was tested in 1 M Na_2SO_4 electrolyte. The CV curves of the NPC//NPC symmetric device (Fig. 5a) were tested at 50 mV s^{-1} in various voltage range. It can be

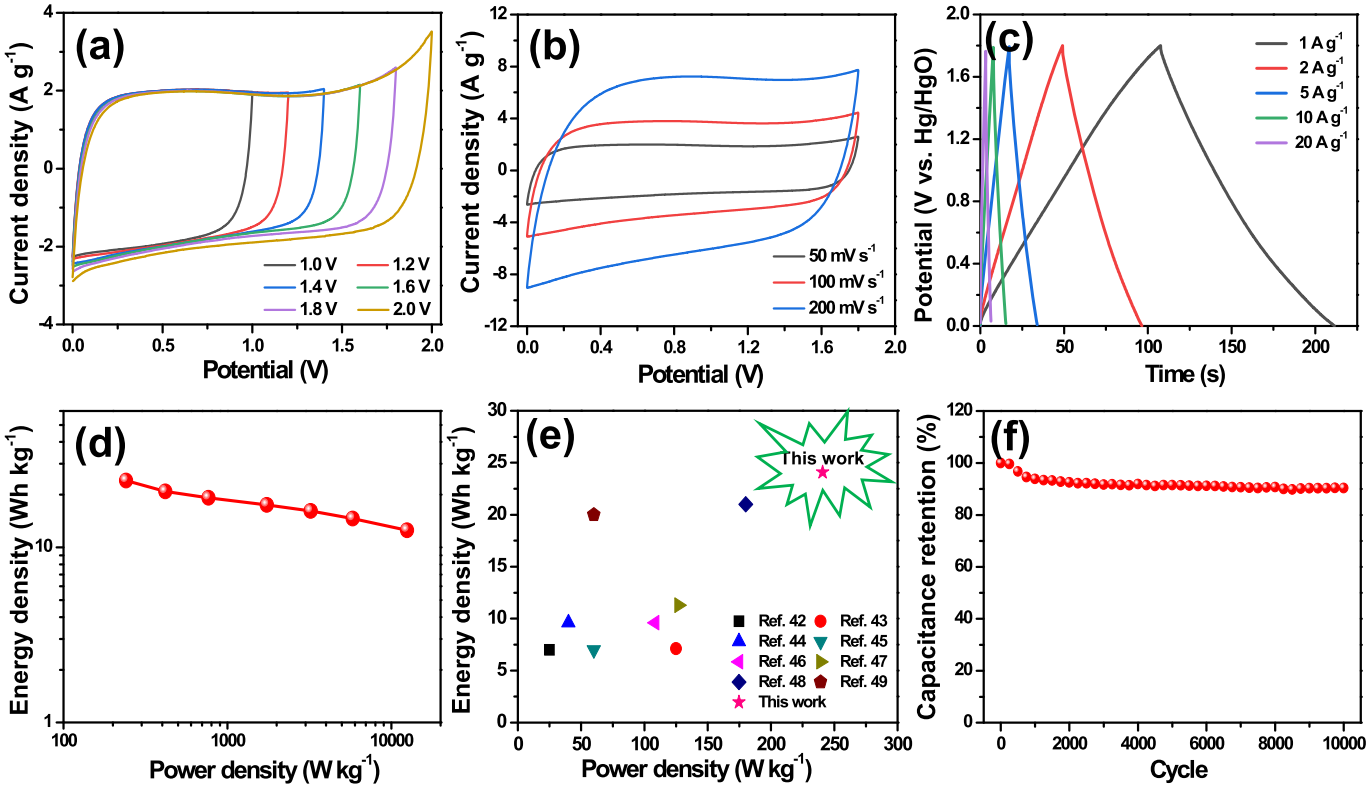

Fig. 5. (**a**) CV curves of the NPC//NPC symmetrical supercapacitor in different operation voltages at a scan rate of 50 mV s^{-1}. (**b**) CV curves of the NPC//NPC symmetrical supercapacitor at different scan rate from 50 to 200 mV s^{-1}. (**c**) Galvanostatic charge/discharge curves of the NPC//NPC symmetrical supercapacitor at various current densities. (**d**) Ragone plots of the NPC//NPC symmetrical supercapacitor and other previously reported carbon based symmetric supercapacitors. (**e**) Performance comparison of the symmetric supercapacitor versus previously reported carbon-based symmetric supercapacitors in aqueous electrolyte. (**f**) Electrochemical stability of the NPC//NPC symmetrical supercapacitor tested at a scan rate of 200 mV s^{-1} for 10,000 cycles.

observed that no obvious increase of anodic current in the voltage window ranging from 0 to 1.8 V, showing that such supercapacitor can be tested in this voltage range. As shown in Fig. 5b, the CV profiles of the NPC//NPC symmetric device were performed in the voltage window of 0–1.8 V from 50 to 200 mV s^{-1}. The CV profile displays rectangular-like profile even at 200 mV s^{-1}, demonstrating good rate performance. Galvanostatic charge/discharge curves show highly linear symmetry (Fig. 5c), meaning that the NPC//NPC symmetric device has good electrochemical invertibility and Columbic efficiency. Benefitting from its large specific capacitance and wide operating voltage, the NPC//NPC symmetrical device shows a maximum energy density of 24.1 Wh Kg^{-1} (Fig. 5d), higher than those of previously reported carbon-based symmetrical supercapacitors (Fig. 5e), such as hierarchical microporous/mesoporous carbon nanosheets [42], nitrogen-doped porous carbon nanofibers [43], graphene nanocapsules [44], porous carbon shell [45], hierarchical porous carbon [46], hollow carbon spheres [47], template carbons [48] and N and S co-doped porous carbon nanosheets [49]. Additionally, the electrochemical stability of the NPC//NPC symmetrical supercapacitor was performed at 200 mV s^{-1} for 10,000 cycles in 1 M Na_2SO_4 solution. It can retain 90.4% of its initial capacitance after 10,000 cycles (Fig. 5f), indicating good cycling stabilization.

All of above results suggest that the NPC material has excellent electrochemical properties for supercapacitors. The excellent electrochemical characteristics of the NPC sample are ascribed to the 3D interconnected porous framework with high surface area and heteroatoms functional groups. Firstly, large specific surface area provides massive active sites to adsorb a great deal of charges and thus in favor of high specific capacity. Secondly, 3D interconnected porous framework not only offers a continuous electronic diffusion route to ensure good electronic contact, but also in favor of ion diffusion by shortening transport path. Finally, heteroatom functional groups can not only improve wettability of NPC, but also provide additional pseudocapacitance during charge-discharge process.

4. Conclusions

In this paper, we develop a facile, one-step way for the synthesis of nitrogen doped porous carbon with 3D interconnected porous structures by one-step pyrolysis of the mixture of agar, potassium citrate and urea. Benefitting from its large specific surface area, 3D interconnected porous framework and heteroatoms functional groups, the NPC materials show large specific capacity, excellent rate performance and good cycling stabilization. Moreover, the as-prepared NPC//NPC symmetric supercapacitor exhibits a high energy density of 24.1 Wh Kg^{-1} in the voltage window of 0–1.8 V in 1 M Na_2SO_4 aqueous solution.

Acknowledgements

Xin Hu and Yahui Wang contributed equally to this work. All authors are very grateful for the financial support of the National Natural Science Foundation of China (51702043), Heilongjiang Postdoctoral Foundation (LBH-Z18008).

Appendix A. Supplementary data

Supplementary data to this article can be found online at https://doi.org/10.1016/j.jallcom.2019.01.160.

References

[1] Y. Wang, Y. Song, Y. Xia, Electrochemical capacitors: mechanism, materials, systems, characterization and applications, Chem. Soc. Rev. 45 (2016) 5925–5950.
[2] F. Béguin, V. Presser, A. Balducci, E. Frackowiak, Carbons and electrolytes for advanced supercapacitors, Adv. Mater. 26 (2014) 2219–2251.
[3] Q. Wang, J. Yan, Z.J. Fan, Carbon materials for high volumetric performance supercapacitors: design, progress, challenges and opportunities, Energy Environ. Sci. 9 (2016) 729–762.
[4] X.L. Wu, L.L. Jiang, C.L. Long, T. Wei, Z.J. Fan, Dual support system ensuring porous Co–Al hydroxide nanosheets with ultrahigh rate performance and high energy density for supercapacitors, Adv. Funct. Mater. 25 (2015) 1648–1655.
[5] X.H. Zhou, L. Cao, Z.H. Li, M.L. Zhang, W.M. Kang, B.W. Cheng, Biomass derived nitrogen-doped hierarchical porous carbon sheets for supercapacitors with high performance, J. Colloid Interface Sci. 523 (2018) 133–143.
[6] M. Sevilla, A. Fuertes, Direct synthesis of highly porous interconnected carbon nanosheets and their application as high performance supercapacitors, ACS Nano 8 (2014) 5069–5078.
[7] Q. Yao, H. Wang, C. Wang, C. Jin, Q. Sun, One step construction of nitrogen–carbon derived from bradyrhizobium japonicum for supercapacitor applications with a soybean leaf as a separator, ACS Sustain. Chem. Eng. 6 (2018) 4695–4704.
[8] D. Guo, B. Ding, X. Hu, Y.H. Wang, F.Q. Han, X.L. Wu, Synthesis of boron and nitrogen codoped porous carbon foam for high performance supercapacitors, ACS Sustain. Chem. Eng. 6 (2018) 11441–11449.
[9] S. Gao, Y. Tang, L. Wang, L. Liu, Z. Sun, S. Wang, H. Zhao, L. Kong, D. Jia, Coal-based hierarchical porous carbon synthesized with a soluble salt self-assembly-assisted method for high performance supercapacitors and Li-ion batteries, ACS Sustain. Chem. Eng. 6 (2018) 3255–3263.
[10] L. Zhang, X. Zhao, Carbon-based materials as supercapacitor electrodes, Chem. Soc. Rev. 38 (2009) 2520–2531.
[11] Y. Zhong, X.H. Xia, S.J. Deng, D. Xie, S.H. Shen, K.L. Zhang, W.H. Guo, X.L. Wang, J.P. Tu, Adv. Mater. 30 (2018), 1805165.
[12] J. Zhang, W. Zhang, H. Zhang, J. Pang, G. Cao, M. Han, Y. Yang, A novel synthesis of hierarchical porous carbons from resol by potassium acetate activation for high performance supercapacitor electrodes, J. Alloys Compd. 712 (2017) 76–81.
[13] Y. Li, Y. Pi, L. Lu, S. Xu, T. Ren, Hierarchical porous active carbon from fallen leaves by synergy of K_2CO_3 and their supercapacitor performance, J. Power Sources 299 (2015) 519–528.
[14] Y. Jiang, J. Yan, X.L. Wu, D. Shan, Q. Zhou, L.L. Jiang, D. Yang, Z.J. Fan, Facile synthesis of carbon nanofibers-bridged porous carbon nanosheets for high-performance supercapacitors, J. Power Sources 307 (2016) 190–198.
[15] H. Luo, Y. Yang, X. Zhao, J. Zhang, Y. Chen, 3D sponge-like nanoporous carbons via a facile synthesis for high-performance supercapacitors: direct carbonization of tartrate salt, Electrochim. Acta 169 (2015) 13–21.
[16] B. Xu, D.F. Zheng, M.Q. Jia, G.P. Cao, Y.S. Yang, Nitrogen-doped porous carbon simply prepared by pyrolyzing a nitrogen-containing organic salt for supercapacitors, Electrochim. Acta 98 (2013) 176–182.
[17] L. Qie, W. Chen, H. Xu, X. Xiong, Y. Jiang, F. Zou, X. Hu, Y. Xin, Z. Zhang, Y. Huang, Synthesis of functionalized 3D hierarchical porous carbon for high-performance supercapacitors, Energy Environ. Sci. 6 (2013) 2497–2504.
[18] X.J. He, Z.D. Liu, H. Ma, N. Zhang, M.X. Yu, M.B. Wu, Shell-like hierarchical porous carbons for high-rate performance supercapacitors, Microporous Mesoporous Mater. 236 (2016) 134–140.
[19] S. Dutta, A. Bhaumik, K.C.W. Wu, Hierarchically porous carbon derived from polymers and biomass: effect of interconnected pores on energy applications, Energy Environ. Sci. 7 (2014) 3574–3592.
[20] X. Hu, X.H. Xu, R.Q. Zhong, L.J. Shang, H.T. Ma, X.L. Wu, P.Y. Jia, Facile synthesis of microporous carbons with three-dimensional honeycomb-like porous structure for high performance supercapacitors, J. Electroanal. Chem. 823 (2018) 54–60.
[21] Y. Lv, L. Gan, M. Liu, W. Xiong, Z. Xu, D. Zhu, D. Wright, A self-template synthesis of hierarchical porous carbon foams based on banana peel for supercapacitor electrodes, J. Power Sources 209 (2012) 152–157.
[22] X.H. Xia, S.J. Deng, S.S. Feng, J.B. Wu, J.P. Tu, Hierarchical porous $Ti_2Nb_{10}O_{29}$ nanospheres as superior anode materials for lithium ion storage, J. Mater. Chem. A 5 (2017) 21134–21139.
[23] T. Wei, X. Wei, Y. Gao, H. Li, Large scale production of biomass-derived nitrogen-doped porous carbon materials for supercapacitors, Electrochim. Acta 169 (2015) 186–194.
[24] J.J. Liu, Y.F. Deng, X.H. Li, L.F. Wang, Promising nitrogen-rich porous carbons derived from one-step calcium chloride activation of biomass-based waste for high performance supercapacitors, ACS Sustain. Chem. Eng. 4 (2015) 177–187.
[25] G. Ma, Q. Yang, K. Sun, H. Peng, F. Ran, X. Zhao, Z. Lei, Nitrogen-doped porous carbon derived from biomass waste for high-performance supercapacitor, Bioresour. Technol. 197 (2015) 137–142.
[26] X.L. Wu, L.L. Jiang, C.L. Long, Z.J. Fan, From flour to honeycomb-like carbon foam: carbon makes room for high energy density supercapacitors, Nano Energy 13 (2015) 527–536.
[27] A. Ferrari, J. Robertson, Interpretation of Raman spectra of disordered and amorphous carbon, Phys. Rev. B 61 (2000) 14095–14107.
[28] S. Stankovich, D. Dikin, R. Piner, K. Kohlhaas, A. Kleinhammes, Y. Jia, Y. Wu, S. Nguyen, R. Ruoff, Synthesis of graphene-based nanosheets via chemical reduction of exfoliated graphite oxide, Carbon 45 (2007) 1558–1565.

[29] Z. Lin, G. Waller, Y. Liu, M. Liu, C. Wong, Facile synthesis of nitrogen-doped graphene via pyrolysis of graphene oxide and urea, and its electrocatalytic activity toward the oxygen-reduction reaction, Adv. Energy Mater. 2 (2012) 884–888.
[30] J. Han, G. Xu, B. Ding, J. Pan, H. Dou, D.R. MacFarlane, Porous nitrogen-doped hollow carbon spheres derived from polyaniline for high performance supercapacitors, J. Mater. Chem. A 2 (2014) 5352–5357.
[31] C.L. Long, L.L. Jiang, X.L. Wu, Y.T. Jiang, D. Yang, C. Wang, T. Wei, Z.J. Fan, Facile synthesis of functionalized porous carbon with three-dimensional interconnected pore structure for high volumetric performance supercapacitors, Carbon 93 (2015) 412–420.
[32] G. Lin, R. Ma, Y. Zhou, Q. Liu, X. Dong, J. Wang, KOH activation of biomass-derived nitrogen-doped carbons for supercapacitor and electrocatalytic oxygen reduction, Electrochim. Acta 261 (2018) 49–57.
[33] L. Sun, C. Tian, Y. Yang, J. Yin, L. Wang, H. Fu, Nitrogen-doped porous graphitic carbon as an excellent electrode material for advanced supercapacitors, Chem. Eur. J. 20 (2014) 564–574.
[34] G. Ma, F. Ran, H. Peng, K. Sun, Z. Zhang, Q. Yang, Z. Lei, Nitrogen-doped porous carbon obtained via one-step carbonizing biowaste soybean curd residue for supercapacitor application, RSC Adv. 5 (2015) 83129–83138.
[35] X. Deng, B. Zhao, L. Zhu, Z. Shao, Molten salt synthesis of nitrogen-doped carbon with hierarchical pore structures for use as high-performance electrodes in supercapacitors, Carbon 93 (2015) 48–58.
[36] K. Xie, X.T. Qin, X.Z. Wang, Y.N. Wang, H.S. Tao, Q. Wu, L.J. Yang, Z. Hu, Carbon nanocages as supercapacitor electrode materials, Adv. Mater. 24 (2012) 347–352.
[37] Z. Li, L. Zhang, B.S. Amirkhiz, X. Tan, Z. Xu, H. Wang, B.C. Olsen, C.M.B. Holt, D. Mitlin, Carbonized chicken eggshell membranes with 3D architectures as high-performance electrode materials for supercapacitors, Adv. Energy Mater. 2 (2012) 431–437.
[38] L. Sun, C. Tian, M. Li, X. Meng, L. Wang, R. Wang, J. Yin, H. Fu, From coconut shell to porous graphene-like nanosheets for high-power supercapacitors, J. Mater. Chem. A 1 (2013) 6462–6470.
[39] H. Zhu, X. Wang, F. Yang, X. Yang, Promising carbons for supercapacitors derived from fungi, Adv. Mater. 23 (2011) 2745–2748.
[40] M. Kwak, A. Ramadoss, K. Yoon, J. Park, P. Thiyagarajan, J. Jang, Single-step synthesis of N-doped three-dimensional graphitic foams for high-performance supercapacitors, ACS Sustain. Chem. Eng. 5 (2017) 6950–6957.
[41] J. Yan, Q. Wang, C. Lin, T. Wei, Z.J. Fan, Interconnected frameworks with a sandwiched porous carbon layer/graphene hybrids for supercapacitors with high gravimetric and volumetric performances, Adv. Energy Mater. 4 (2014), 1400500.
[42] A. Fuertes, M. Sevilla, Hierarchical microporous/mesoporous carbon nanosheets for high performance supercapacitors, ACS Appl. Mater. Interfaces 7 (2015) 4344–4353.
[43] L. Chen, X. Zhang, H. Liang, M. Kong, Q. Guan, P. Chen, Z. Wu, S. Yu, Synthesis of nitrogen-doped porous carbon nanofibers as an efficient electrode material for supercapacitors, ACS Nano 6 (2012), 7902-7102.
[44] X. He, X. Li, H. Ma, J. Han, H. Zhang, C. Yu, N. Xiao, J. Qiu, ZnO template strategy for the synthesis of 3D interconnected graphene nanocapsules from coal tar pitch as supercapacitor electrode materials, J. Power Sources 340 (2017) 183–191.
[45] W. Yang, W. Yang, F. Ding, L. Sang, Z. Ma, G. Shao, Template-free synthesis of ultrathin porous carbon shell with excellent conductivity for high-rate supercapacitors, Carbon 111 (2017) 419–427.
[46] Q. Wang, J. Yan, Y. Wang, T. Wei, M. Zhang, X. Jing, Z.J. Fan, Three-dimensional flower-like and hierarchical porous carbon materials as high-rate performance electrodes for supercapacitors, Carbon 67 (2014) 119–127.
[47] Q. Wang, J. Yan, Y. Wang, G. Ning, Z.J. Fan, T. Wei, J. Cheng, M. Zhang, X. Jing, Template synthesis of hollow carbon spheres anchored on carbon nanotubes for high rate performance supercapacitors, Carbon 52 (2013) 209–218.
[48] E. Frackowiak, G. Lota, J. Machnikowski, C. Vix-Guterl, F. Beguin, Optimisation of supercapacitors using carbons with controlled nanotexture and nitrogen content, Electrochim. Acta 51 (2006) 2209–2214.
[49] Y. Li, G. Wang, T. Wei, Z.J. Fan, P. Yan, Nitrogen and sulfur co-doped porous carbon nanosheets derived from willow catkin for supercapacitors, Nano Energy 19 (2016) 165–175.